

On the selective magnetic induction heating of micron scale structures

This article has been downloaded from IOPscience. Please scroll down to see the full text article.

2006 J. Micromech. Microeng. 16 1314

(<http://iopscience.iop.org/0960-1317/16/7/028>)

View [the table of contents for this issue](#), or go to the [journal homepage](#) for more

Download details:

IP Address: 140.114.59.160

The article was downloaded on 21/08/2012 at 05:43

Please note that [terms and conditions apply](#).

On the selective magnetic induction heating of micron scale structures

Hsueh-An Yang¹, Chiung-Wen Lin², Chih-Yu Peng² and Weileun Fang^{1,2}

¹ Power Mechanical Engineering Department, National Tsing Hua University, Hsinchu 30043, Taiwan

² MEMS Institute, National Tsing Hua University, Hsinchu 30043, Taiwan

E-mail: fang@pme.nthu.edu.tw

Received 21 March 2006, in final form 18 April 2006

Published 23 May 2006

Online at stacks.iop.org/JMM/16/1314

Abstract

Magnetic induction heating is a promising heating approach for MEMS processes and devices. This study has discussed the scale effect of induction heating for thin-film microstructures through analytical and experimental means. The results show that the temperature increase varies with the in-plane surface area of the microstructure and the relative permeability of thin-film materials. Moreover, the shape of the microstructure also leads to the difference of temperature increase. In applications, localized heating and various temperature regions can be simultaneously achieved on the substrate by applying an external high-frequency magnetic field.

(Some figures in this article are in colour only in the electronic version)

1. Introduction

Magnetic induction heating is a simple yet cost-effective heating approach. It is a popular technology to quickly produce a temperature rise in some bulk materials [1]. This technology has been extensively employed to heat electrically conductive materials for various applications such as melting, soldering and hardening of metals. As shown in figure 1(a), the induction heating system consists of a high-frequency power supply, an induction coil and the macro workpiece. The ac power supply is exploited to drive the induction coil to generate a magnetic field. As a macro workpiece is placed in the magnetic field, the eddy current is induced close to the surface of the specimen. Thus, most of the heat will be generated within the macro workpiece due to the eddy current loss and hysteresis loss, as indicated in figure 1(a) [2]. The induction heating region in the workpiece is determined by the skin effect [3]. In general, the macro workpiece to be heated is larger than the induction heating region. Tuning the dimensions of the macro workpiece will not influence the size of the induction heating region.

Presently, magnetic induction heating has also demonstrated applications in thin-film devices and microelectromechanical systems [4, 5]. The dimensions of a thin-film microstructure are much smaller than those of the bulk one, hence the scale effect of induction heating needs to

be investigated. Because of the skin effect, induction heating is localized on the surface of the macro workpiece. However, the thickness of a thin-film microstructure is even smaller than that of the skin depth, as shown in figure 1(b). Figure 1(b) also indicates that the surface area (in-plane dimensions) of the micro workpiece is smaller than that of the magnetic field. Thus, the eddy current will be induced not only near the surface but also on the whole of the micro workpiece, and magnetic induction heating will directly heat the whole micro workpiece. Moreover, a variation of micro workpiece dimensions will influence the size of the induction heating region.

As a result, the in-plane dimensions of the micro workpiece will significantly influence the heat flux and the temperature change of induction heating. This study has fabricated thin-film microstructures on silicon substrate to act as micro workpieces. By varying the dimensions of the micro workpieces, selective induction heating for thin-film microstructures is investigated through analytical and experimental means.

2. Concept

This study considers the induction heating of thin-film micro workpieces, as illustrated in figure 1(b), in a magnetic field

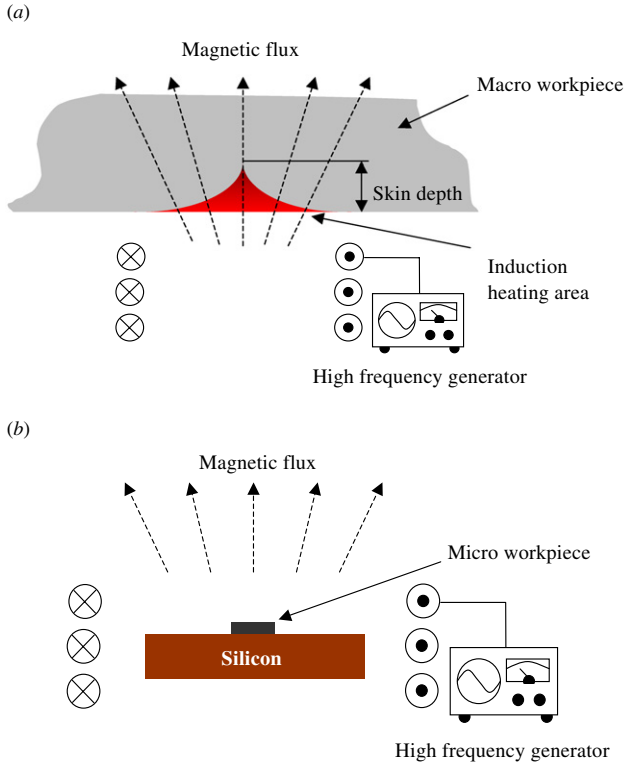


Figure 1. Schematic illustration of induction heating for (a) the macro workpiece and (b) the micro workpiece. The workpiece was placed inside a magnetic field provided by the coil underneath.

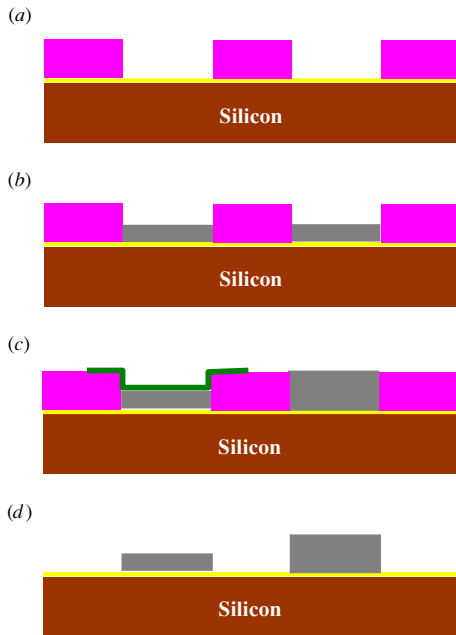


Figure 2. The fabrication process to prepare the micro workpiece of the present study.

with an operating frequency f and intensity H . In this case, the micro workpiece is fully covered by the magnetic field, and A_s is the in-plane surface area of the thin-film microstructures orthogonal to the magnetic flux. Hence, the variation of the surface area A_s of the micro workpiece will change the

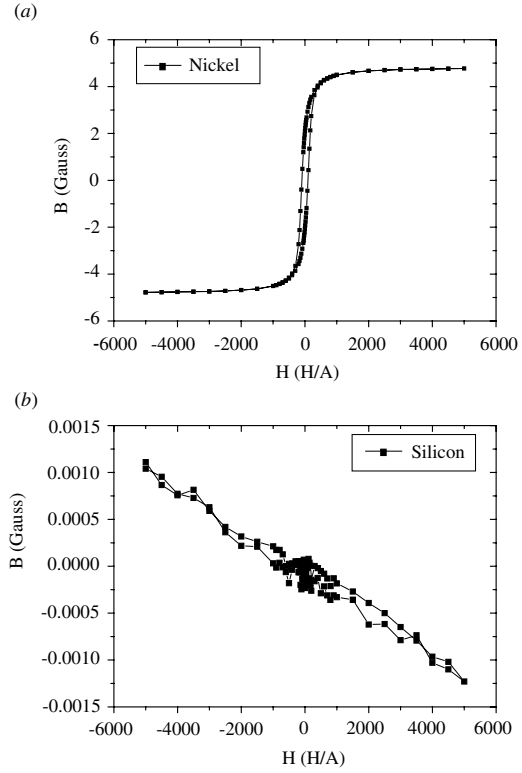


Figure 3. The measured B-H loops using a vibrating sample magnetometer for (a) Ni film and (b) Si substrate.

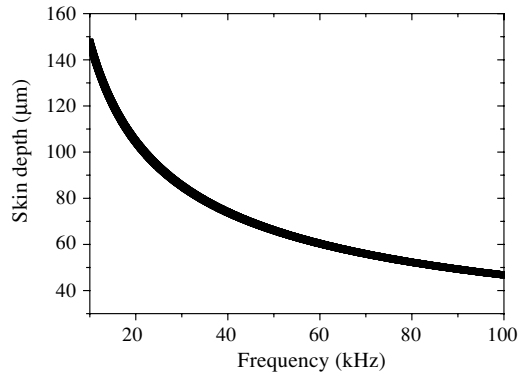


Figure 4. The predicted variation of the skin depth with the operation frequency of the magnetic field.

induction heating region. The thin-film material has a relative permeability μ_r , and an electrical resistivity ρ . By ignoring the heat transfer between the thin film and the substrate, the temperature increase ΔT of the microstructure due to the induction heating of time t is expressed as [6, 7]

$$\Delta T \propto C A_s \frac{\mu_r^2}{\rho} f^2 H^2 t, \quad (1)$$

where C is the geometry constant determined by the in-plane shape (e.g. circle, square, triangle, etc) of the thin-film microstructure.

According to equation (1), the temperature increase ΔT varies with the surface area A_s of the heating micro workpiece. Thus, the temperature increase ΔT can be tuned by varying

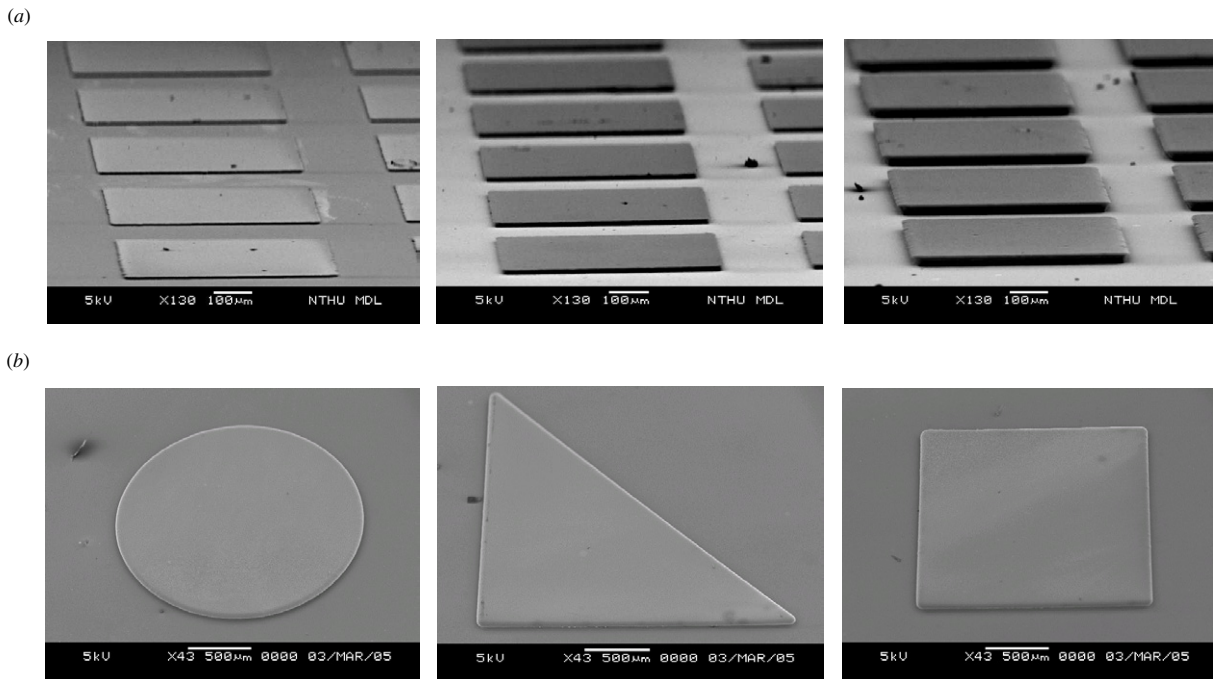


Figure 5. SEM photographs of some typical fabricated micro workpieces with (a) different thicknesses and (b) different in-plane shapes.

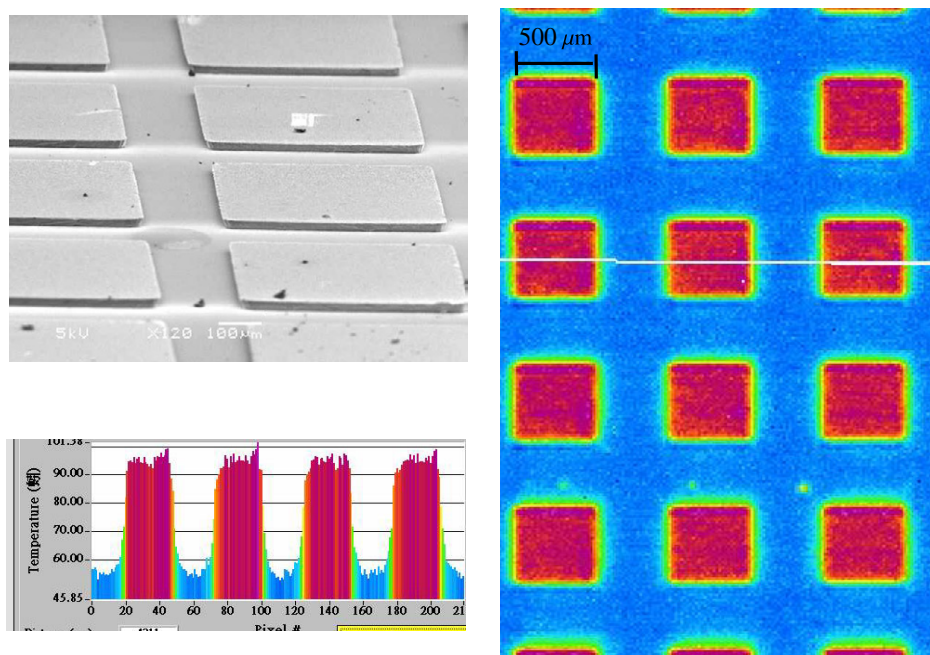


Figure 6. The typical measured temperature distribution displayed by the infrared microscope.

not only the power of the magnetic field (i.e. f and H) but also the planar dimensions (length and width) of the micro workpiece. However, the induction heating regions of the macro workpiece will not be influenced by varying its size. Thus, the temperature increase ΔT from induction heating can only be tuned by varying the power of the magnetic field. Moreover, thin-film materials with different relative permeabilities μ_r as well as electrical resistivity ρ have different temperature increases during induction heating. In short, selective heating on a silicon substrate can be achieved

by means of tuning the in-plane pattern as well as changing the materials of the thin films.

Moreover, the variation of temperature increase with film thickness of the micro workpiece has also been investigated by finite element simulation. The heat transfer between the micro workpiece and the silicon substrate is considered in the finite element model. According to equation (1), the film thickness will not affect the temperature increase after ignoring the heat transfer. However, for micro structures with the same surface area, the thicker one will generate more total heat during

Table 1. The recipe of electroplating solutions for the Ni film.

Nickel sulfamate $\text{Ni}(\text{NH}_2\text{SO}_4)_2 \cdot 4\text{H}_2\text{O}$	450–550 g l ⁻¹
Nickel chloride $\text{NiCl}_2 \cdot 6\text{H}_2\text{O}$	2–7 g l ⁻¹
Bromic acid H_3BO_3	30–50 g l ⁻¹
Stress reducer	2–10 ml l ⁻¹

induction heating. Thus, a micro workpiece with a thicker film produces a higher temperature increase after considering the heat transfer at the boundary of the film and the substrate. Selective heating on a silicon substrate can also be achieved by means of tuning the film thickness.

3. Experiments

In the experiment, LIGA-like processes were employed to fabricate and pattern the thin-film microstructures on the silicon substrate. As shown in figure 2(a), the process began with photolithography of a 20 μm thick AZP-4620 resist. After that, the thin film was electroplated on the top of the silicon substrate, as shown in figure 2(b). The electroplated film formed the test micro workpiece after removing the photo resist. Nickel film (ferromagnetic material) with higher relative permeability μ_r was selected for the present test. To prepare the micro workpiece, the nickel had various electroplated film thicknesses. In addition, the nickel film was patterned into various in-plane surface areas and shapes (including circles, triangles and squares). As illustrated in figures 2(c)–(d), this study also employed tape to selectively deposit the test micro workpiece with different thicknesses after the second electroplating. In the present study, the thickness uniformity and surface roughness of the electroplated film were carefully controlled by the current density during the electroplating process [8]. The recipe of electroplating solutions of nickel is shown in table 1. As a result, the thickness variation of the electroplated film was less than 0.2 μm . Moreover, the surface roughness of the film was near 20–40 nm.

The measured B-H loops (or hysteresis curve) for the Si substrate and the Ni film respectively using a VSM (vibrating sample magnetometer) are shown in figure 3. It shows that the Ni film has a much higher relative permeability than the Si substrate. The operating frequency and the power of the magnetic field were 82 kHz and 30 kW, respectively. Figure 4 shows the variation of skin depth with the operation frequency of the magnetic field predicted by [9]. Consequently, the skin depth of the nickel film (μ_r and $1/\rho$ are 100 and $1.16 \times 10^7 \text{ S m}^{-1}$, respectively) associated with the operating frequency of 82 kHz was 54 μm . The thickness of the electroplated nickel film was selected to be 10 μm to prevent the increase of skin depth. The substrate and nickel film microstructures were then induction heated using the test setup shown in figure 1(b). The temperature distribution of the silicon substrate and the micro workpiece was measured using an infrared microscope during the induction heating. The spatial resolution ranges from 3 μm to 60 μm and the temperature resolution of the infrared thermal microscope is 0.1 $^\circ\text{C}$. Thus, the selective magnetic induction heating of the micro workpiece can be characterized using these test structures.

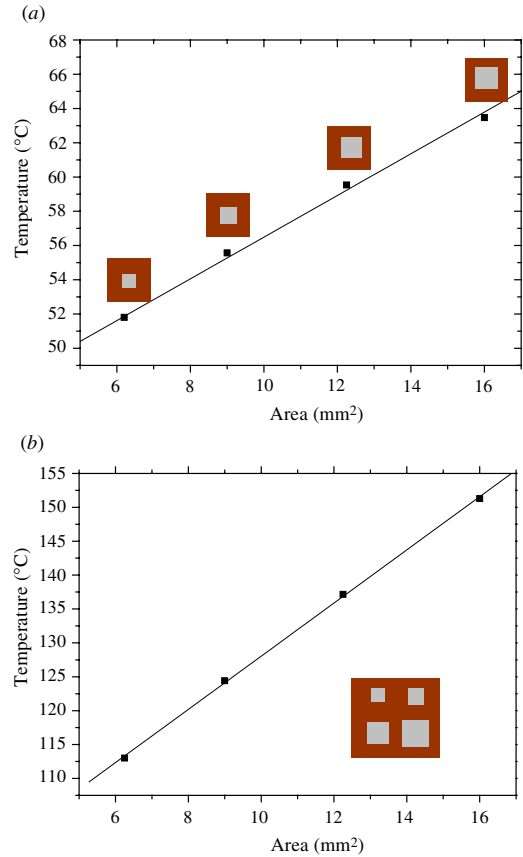


Figure 7. The measured temperature increase of four different square nickel patterns when induction heated by the magnetic field (a) individually and (b) simultaneously.

4. Results and discussions

The SEM photographs in figure 5(a) show typical test structures, and the thicknesses of these structures are 5.2 μm , 11.3 μm and 27.3 μm , respectively. The SEM photographs in figure 5(b) show typical test structures with circles, triangles and square shapes, respectively. The surface areas of these micro workpieces are 9 mm² and 16 mm², respectively. Figure 6 demonstrates the typical measured temperature distribution displayed by the infrared microscope. In this case, the colors represent the temperatures of the silicon substrate and square nickel pattern array during induction heating. Thus, the selective magnetic induction heating of the micro workpiece on the silicon substrate was characterized.

4.1. Selective induction heating—material effect

According to equation (1), the temperature increase due to the induction heating is significantly influenced by the relative permeability μ_r of a material. In this experiment, the ferromagnetic Ni film has μ_r of 100 and μ_r of a diamagnetic Si substrate is slightly less than 1. The operating frequency of the present induction heating was only 82 kHz to heat the Ni film with high relative permeability; meanwhile the silicon substrate had a smaller temperature rise. The measurement results in figure 6 show that the high-temperature area (nickel) was above 90 $^\circ\text{C}$ and the low-temperature area (silicon)

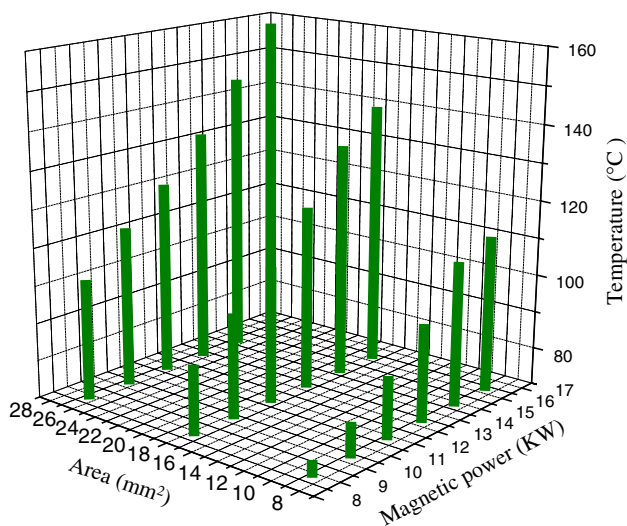


Figure 8. The measured variation of temperature increase ΔT with the input power and the area A_s of nickel patterns.

substrate) was near 45 °C after induction heating for 10 s. Thus, heating selectivity between the silicon substrate and the deposited films is obtained. As a comparison, induction heating was operated in a frequency range of 13.6 MHz to

2.45 GHz in [10] to heat the silicon substrate. This characteristic can be exploited to perform a localized heating source on the silicon substrate.

4.2. Selective induction heating—geometric (size and shape) effects

This study has characterized the variation of the temperature increase ΔT on the area A_s . The power output from the high-frequency generator was near 15 kW. Figure 7(a) indicates the measured temperature increase of four different square nickel patterns when they were induction heated individually. The heating area A_s of these four patterns ranged from 6 mm² to 16 mm², and the heating time was 15 s. The measured results in figure 7(a) agree with the linear relation of A_s and T predicted in equation (1). Besides, the test to heat the chip containing all these four nickel patterns was also available. Figure 7(b) indicates the temperature increase of these nickel patterns after they were induction heated simultaneously by the magnetic field. The measured results indicate that each nickel pattern experienced a significant temperature change, as compared with the results in figure 7(a). This effect results from the increase of the net magnetic flux density. The measurement results regarding the variation of T with input power and the area A_s of nickel patterns are summarized in figure 8.

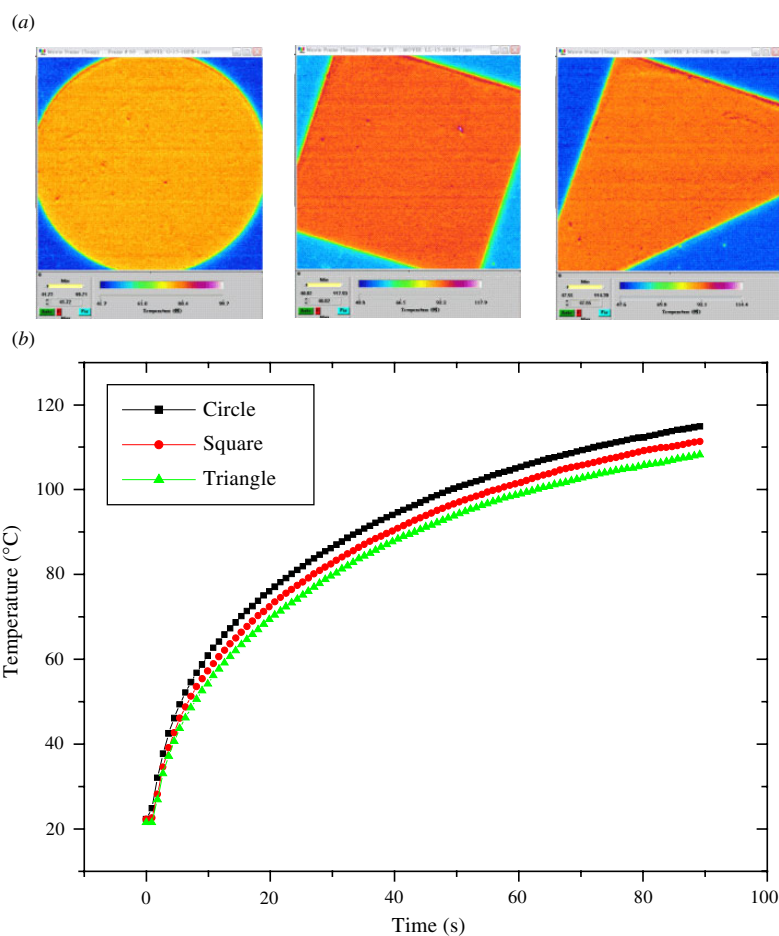


Figure 9. (a) Thermal images and (b) variation of the temperature increase with time of nickel patterns with three different in-plane shapes measured by the infrared microscope.

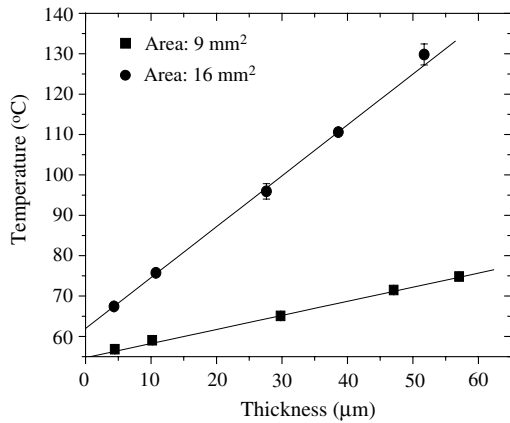


Figure 10. The temperature increase of nickel patterns with five different thicknesses.

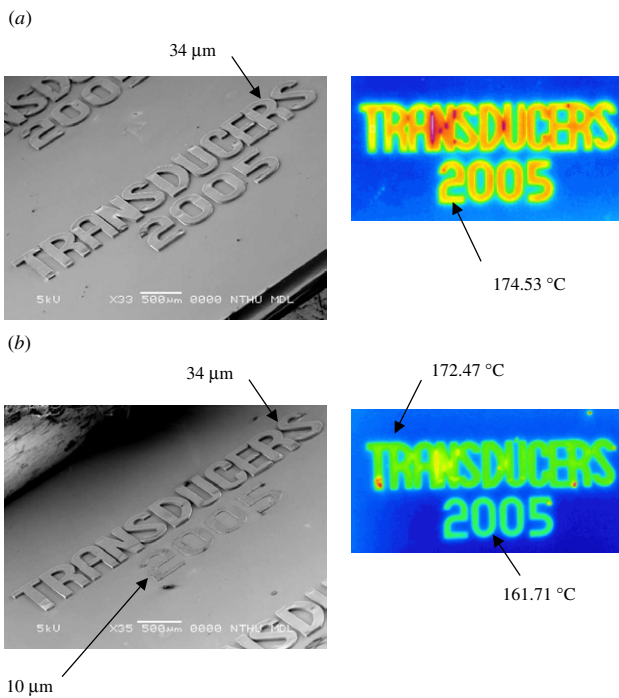


Figure 11. Measured thermal images of the words 'TRANSDUCERS 2005' (a) with the same thickness of 34 μm and (b) 10 μm thick for '2005' and 34 μm thick for 'TRANSDUCERS'.

It indicates that the temperature increase of induction-heated microstructures can be tuned by varying the area of A_s or by adjusting the power of the high-frequency generator. These characteristics can be exploited to provide selective induction heating on the silicon substrate.

The variation of temperature increase with the in-plane shape of the nickel pattern was also investigated. This study designed three patterns with the same area A_s but different in-plane shapes (including circles, squares and triangle shapes), as shown in figure 5(b). However, it is expected that the shape of the nickel pattern will influence the path of the eddy current. This characteristic has been taken into consideration in the geometry constant C of equation (1). Figure 9(a) shows the thermal images of these nickel patterns measured by the

infrared microscope. The surface area A_s of these patterns was 20.25 mm², and the thickness h was 10 μm. The temperature increase in these three patterns is 115 °C (circles), 111 °C (squares) and 108 °C (triangles), respectively, after heating for 90 s. As a comparison, the geometry constant of these patterns was $C_{\text{circle}} > C_{\text{square}} > C_{\text{triangle}}$; hence, the measurement results in figure 9(b) roughly followed the trend predicted by equation (1).

Finally, the variation of film thickness and temperature increase has also been studied. In this experiment, nickel films with thicknesses ranging from 4 μm to 53 μm were electroplated. The temperature increase was characterized after the test structures were induction heated for 20 s. The power of the high-frequency generator was 30 kW. Figure 10 indicates the temperature increase of nickel patterns with five different thicknesses. The trend in figure 10 follows the results predicted by finite element simulation. Moreover, the test nickel patterns contained two different surface areas (16 mm² and 9 mm², respectively). Once again, the pattern with a larger surface area had a higher temperature increase. Figure 11 shows the words of 'TRANSDUCERS 2005'. The words in figure 11(a) have the same electroplating thickness of 34 μm and their measured temperatures were all 174.53 °C after induction heating. However, the thickness of the words in figure 11(b) is 10 μm (for '2005') and 34 μm (for 'TRANSDUCERS'), respectively. The measured temperatures were 161.71 °C for '2005' and 172.47 °C for 'TRANSDUCERS' after the induction heating.

5. Conclusions

Magnetic induction heating is a rapid and non-contact heating technology. This study presents the selectivity of magnetic induction heating for thin-film microstructures. The relative permeability of a material is the most important characteristic to tune the heating selectivity. Thus, localized heating can be easily realized on the silicon substrate (diamagnetic material) by means of ferromagnetic thin films (Ni, Fe, etc). Moreover, the surface area of the micro pattern orthogonal to the magnetic field would dominate the magnetic flux in the microscale. In this regard, the in-plane dimensions of the thin-film microstructure will significantly influence the temperature change of induction heating. The shape of the microstructure will also influence the path of the eddy current, so as to vary the temperature increase of induction heating. These characteristics can be exploited to tune the temperature increase of microstructures by merely varying their in-plane dimensions. Since it is easy to employ the photolithography process to define the planar dimensions of microstructures, selective magnetic induction heating is easily achieved for micro devices.

Acknowledgments

This project was (partially) supported by the NSC of Taiwan under grant NSC-93-2218-E-007-012 and the Ministry of Economic Affairs, Taiwan, under contract 93-EC-17-A-07-S1-0011. The authors would also like to thank the NSC Central

Regional MEMS Center (Taiwan), the Nano Facility Center of the National Tsing Hua University and the NSC National Nano Device Laboratory (NDL) for providing the fabrication facilities.

References

- [1] John D and Peter S 1979 *Induction Heating Handbook* (New York: McGraw-Hill)
- [2] Cullity B D 1972 *Introduction to Magnetic Materials* (Boston, MA: Addison-Wesley)
- [3] Stansel N R 1949 *Induction Heating* (New York: McGraw-Hill)
- [4] Yang H A, Lin C W and Fang W 2006 Wafer level self-assembly of microstructures using global magnetic lifting and localized induction welding *J. Micromech. Microeng.* **16** 27–32
- [5] Yang H A, Wu M C and Fang W 2005 Localized induction heating solder bonding for wafer level MEMS packaging *J. Micromech. Microeng.* **15** 394–9
- [6] Guy A G 1976 *Essentials of Materials Science* (New York: McGraw-Hill)
- [7] Jackson J D 1975 *Classical Electrodynamics* 2nd edn (New York: Wiley)
- [8] Romankiw L T 1997 A path: from electroplating through lithographic masks in electronics to LIGA in MEMS *Electrochim. Acta* **42** 2985–3005
- [9] Johnson H and Graham M 2003 *High-speed Signal Propagation* (Englewood Cliffs, NJ: Prentice-Hall)
- [10] Thompson K, Gianchandani Y, Booske J and Cooper R 2002 Direct silicon–silicon bonding by electromagnetic induction heating *J. Microelectromech. Syst.* **11** 285–92